

2 **Insight into inclusion complexation of indomethacin nicotinamide**
3 **cocrystals**4 Hassan Refat H. Ali¹ · Imran Y. Saleem² · Hesham M. Tawfeek³5 Received: 24 August 2015 / Accepted: 6 January 2016
6 © Springer Science+Business Media Dordrecht 2016

7 **Abstract** The objective of this research was to investi-
8 gate the feasibility of the interaction between
9 indomethacin-nicotinamide cocrystals with β -cyclodextrin
10 and hydroxypropyl- β -cyclodextrin in the solid-state. The
11 study has emphasized on the possibility of inclusion
12 complex formation and its effect on the dissolution per-
13 formance of the cocrystals. The solid systems in the molar
14 ratio of 1:1 of the host and guest molecules were prepared
15 by co-grinding and co-evaporation methods and compared
16 with their physical mixtures. Furthermore, the molecular
17 behaviors of the cocrystals in all prepared samples were
18 thoroughly characterized by powder X-ray diffraction,
19 differential scanning calorimetry, Fourier-transform infra-
20 red spectroscopy, scanning electron microscopy and
21 in vitro dissolution performance. The results of these
22 studies indicated that complexes prepared by the co-evap-
23 oration method with hydroxypropyl- β -cyclodextrin have
24 shown complete inclusion of the cocrystals into the
25 cyclodextrin cavity and a partial inclusion with β -cy-
26 clodextrin. Moreover, a significant ($p < 0.05$; ANOVA/
27 Tukey) higher in vitro dissolution was achieved in co-
28 evaporate complex prepared with hydroxypropyl- β -cy-
29 clodextrin compared to that prepared with β -cyclodextrin,
30 indomethacin-nicotinamide cocrystals and indomethacin
31 itself.

Keywords Cocrystals · β -Cyclodextrins · HP- β - 33
Cyclodextrin · Indomethacin · Inclusion complexation · 34
Nicotinamide 35

Introduction 36

In the development and manufacture of pharmaceutical 37
products, improving the physicochemical properties of 38
drugs is often essential but can be challenging. Because 39
these improvements can often be achieved by making new 40
solid forms of the drug without altering its chemical 41
structure. Recent research has focused on identifying 42
polymorphs, hydrates, solvates, salts and, more recently, 43
cocrystals of drugs [1]. Cocrystals are composed of mul- 44
tiple molecular components, including the drug and a 45
benign, non-toxic ‘coformer’ molecule. The design, for- 46
mation and understanding of the physicochemical 47
properties of cocrystals have received considerable atten- 48
tion [2–5]. Indeed, pharmaceutical cocrystals are an 49
attractive alternative solid form with the potential to fine 50
tune the physicochemical properties of drugs [6]. 51

Inclusion or host–guest complexes are supramolecular 52
systems where one chemical compound (the *host*) has a 53
cavity, in which molecules of a second compound (the 54
guest) are located [7, 8]. The study of non-covalent forces 55
involved in the formation of host–guest complexes is of 56
paramount importance for the design of synthetic inclusion 57
compounds of active pharmaceutical ingredients (APIs). 58

β -Cyclodextrin (β -CD) is a cyclic oligosaccharide con- 59
sisting of seven glucose units linked by α (1 \rightarrow 4) bonds, 60
resulting in a hollow truncated cone shape [9]. In water 61
they have a hydrophilic outer surface and a hydrophobic 62
central cavity able to include a wide variety of lipophilic 63
guest molecules, with suitable polarity and dimensions, 64

A1 ✉ Hassan Refat H. Ali
A2 hareha11374@gmail.com

A3 ¹ Department of Pharmaceutical Analytical Chemistry, Faculty
A4 of Pharmacy, Assiut University, Assiut 71526, Egypt

A5 ² School of Pharmacy and Biomolecular Science, Liverpool
A6 John Moores University, Liverpool, UK

A7 ³ Department of Industrial Pharmacy, Faculty of Pharmacy,
A8 Assiut University, Assiut 71526, Egypt

65 without the formation of any covalent bond [10]. Com-
66 plexation with β -CD has found extensive applications in
67 pharmaceutical technology to enhance the aqueous solu-
68 bility, dissolution rate, bioavailability, and stability of
69 poorly water soluble drugs [11, 12]. Unsubstituted β -CD
70 has poor water solubility (16 mg mL^{-1} at $25 \text{ }^\circ\text{C}$), whereas
71 random substitution of the hydroxyl groups with alkyl or
72 hydroxyalkyl groups is able to increase solubility. There-
73 fore, several synthetically modified β -CDs were used as
74 multifunctional drug carriers in parenteral formulations,
75 such as hydroxypropyl β -cyclodextrin (HP- β -CD) [13].

76 Indomethacin (IND) (1-(p-chlorobenzoyl)-5-methoxy-2-
77 methylindole-3-acetic acid) (Scheme 1a) is a non-steroidal
78 anti-inflammatory drug [14]. It is known to form cocrystals
79 with a non-toxic coformer, nicotinamide (NIC)
80 (Scheme 1b) [15, 16].

81 To the best of our knowledge, indomethacin-nicoti-
82 namide cocrystals (INDNIC) complexation with different
83 cyclodextrins has not been studied before. There is only an
84 available report in the literature about formulation devel-
85 opment of carbamazepine-nicotinamide cocrystals
86 complexed with γ -cyclodextrin using supercritical fluid
87 process [17]. In spite of γ -cyclodextrin is a highly water
88 soluble derivative of cyclodextrins but it is not economic
89 for the pharmaceutical industry. Additionally, the super-
90 critical fluid technology is a complex, expensive and time
91 consuming process. So, the objective of the present work
92 was to study the feasibility of interaction of INDNIC with
93 other types of cyclodextrins e.g., β -CD and HP- β -CD in
94 the solid-state. More economic, simple and fast approaches
95 have been applied to achieve inclusion complex formation
96 which are co-grinding and co-evaporation methods. The
97 study was further aimed to characterize the prepared
98 complexes by powder X-ray diffraction (PXRD), differ-
99 ential scanning calorimetry (DSC), Fourier-transform
100 infrared (FTIR) spectroscopy and scanning electron
101 microscopy (SEM). An in vitro dissolution study was also
102 conducted to show the effect of cocrystals inclusion com-
103 plexation on the dissolution profile of IND after its

104 complexation with cyclodextrins compared with uncom-
105 plexed (free) INDNIC cocrystals and pure IND. **AQ1**

106 Experimental

107 Materials

108 Indomethacin (γ form), nicotinamide, ethyl acetate,
109 methanol were purchased from Sigma-Aldrich (Cairo,
110 Egypt). β -cyclodextrin and HP- β -cyclodextrin were pur-
111 chased from Fluka Chemie (Switzerland). All chemicals
112 and solvents were of analytical grade and used as received.

113 Preparation of indomethacin cocrystals

114 Indomethacin cocrystals were prepared by slurry crystal-
115 lization [18]. A total of approximately 3.578 g of IND and
116 1.221 g of NIC in a (1:1 molar ratio) was magnetically
117 stirred in 10 ml of ethyl acetate for 5 days at room tem-
118 perature. Solids were filtered, dried and analyzed by
119 PXRD, DSC and FTIR.

120 Preparation of the physical mixtures

121 Physical mixtures of INDNIC with β -CD and HP- β -CD in
122 (1:1 molar ratio) were prepared by simple blending in a
123 glass mortar for 5 min and stored under vacuum in desic-
124 cator over calcium chloride for five consecutive days.

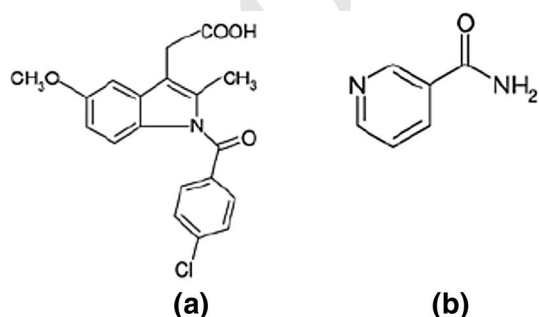
125 Preparation of the inclusion complexes

126 Co-grinding method

127 The ground mixtures of INDNIC with each of β -CD and
128 HP- β -CD in (1:1 molar ratio) were prepared using the
129 vibrational uniball mill (VEB leuchtenbau-KM1, Ger-
130 many) for 15 min. The ground mixtures were sieved to
131 obtain a particle size range of 125–250 μm , and then stored
132 in a desiccator over calcium chloride for five consecutive
133 days.

134 Co-evaporation method

135 Co-evaporates of INDNIC with each of β -CD and HP- β -
136 CD were prepared by solvent evaporation method in the
137 same molar ratio (1:1) as previously reported [19]. Briefly,
138 IND-NIC was dissolved in a sufficient volume of methanol.
139 Both β -CD and HP- β -CD were dissolved at $40 \text{ }^\circ\text{C}$ in dis-
140 tilled water. INDNIC and respective CD solutions were
141 mixed together with constant stirring and kept at $40 \text{ }^\circ\text{C}$
142 for an hour, then gradually cooled to room temperature over a
143 period of 6 h. The solutions were evaporated at $40 \text{ }^\circ\text{C}$ under



Scheme 1 The chemical structures of **a** IND and **b** NIC

144	vacuum till a constant weight was achieved. The collected	186
145	powders were sieved to obtain a particle range of 125–	187
146	250 μm and stored under vacuum in a desiccator over	188
147	calcium chloride for five consecutive days.	189
148	Instrumentation	
149	Powder X-ray diffractometry (PXRD)	
150	The powder X-ray diffraction patterns of the solid samples	191
151	were recorded using a Philips 1710 powder diffractometer	192
152	with Cu $K\alpha$ radiation (1.54056 \AA). A Cu target tube	193
153	operated at a voltage of 40 kV and a current of 40 mA and	194
154	a single crystal graphite monochromator were employed. A	195
155	scanning speed of $0.6^\circ/\text{min}$ and a wide angel diffraction of	196
156	$4^\circ < 2\theta < 60^\circ$ were applied. Standard polycrystalline sili-	197
157	con powder was used to calibrate the instrument.	198
158	Differential scanning calorimetry (DSC)	199
159	DSC thermograms were obtained by using a Shimadzu	200
160	DSC-50 (Japan). Samples of about 5 mg were placed in	201
161	aluminum pans of 50 μL capacity & 0.1 mm thickness,	202
162	press-sealed with aluminum cover of 0.1 mm thickness. An	203
163	empty pan sealed in the same way was used as a reference.	204
164	The thermograms were recorded by heating the samples	205
165	from 30 to 250 $^\circ\text{C}$ at a rate of $10^\circ\text{C min}^{-1}$, under nitrogen	206
166	flow of 40 ml min^{-1} . Indium was used as a standard for	207
167	calibrating the temperature. Reproducibility was checked	208
168	by running the samples in triplicate, the standard deviations	
169	calculated were found negligible.	
170	Infrared spectroscopy	209
171	FT-infrared spectra were collected in triplicate using a	210
172	Nicolet 6700 FTIR Advanced Gold Spectrometer in the	211
173	diffuse reflectance mode with potassium bromide as a	212
174	diluent (1:200), using $<10\text{ mg}$ of the solid samples. The	213
175	spectra were recorded in the range of $400\text{--}4000\text{ cm}^{-1}$ at	214
176	2 cm^{-1} spectral resolution with the accumulation of 256	215
177	spectral scans. The instrument was controlled with OMNIC	216
178	8 software. Triplicate spectra were averaged to obtain one	
179	spectrum for each sample. All FTIR spectra were exported	
180	to the Galactic* SPC format using GRAMS AI (Version	
181	8.0, Thermo Electron Corp. Waltham, MA, USA) with no	
182	further processing.	
183	Scanning electron microscopy	217
184	Particles were visualized by scanning electron microscopy	218
185	(SEM; Jeol 5400 LV, Japan).	219
	Particles were mounted on aluminum stubs (pin stubs,	220
	13 mm), layered with a sticky conductive carbon tab and	221
	coated in gold (10–15 nm) using an EmiTech K 550X Gold	222
	Sputter Coater, 25 mA for 3 min.	223
	In-vitro dissolution	224
	Dissolution experiments were carried out in triplicate with	225
	USP apparatus II dissolution using paddle at a rotation	226
	speed of 100 rpm. Powdered samples of each preparation	227
	equivalent to 25 mg of IND were added to the dissolution	228
	medium, 500 mL of phosphate buffer, pH 7.4, kept at	229
	$37 \pm 0.5^\circ\text{C}$. At appropriate time intervals, 5 mL of the	
	solution were withdrawn using cotton plug from the dis-	
	solution medium and replaced with an equal volume of the	
	fresh dissolution medium equilibrated at 37°C . Then ali-	
	quots were injected into the HPLC system. The HPLC	
	system, Knauer, D-14163, Germany, consists of HPLC	
	pump, UV- detector, and integration interface box. Chro-	
	matographic separation was carried out using Kromasil	
	C-18 column ($250 \times 4.60\text{ mm}$, particle size: $20\text{ }\mu\text{m}$). The	
	detection wavelength, 377 nm, was determined by scan-	
	ning the maximum absorbance wavelength of IND in the	
	mobile phase (Methanol: distilled water) using an UV-Vis	
	spectrophotometer (Jenway, Model 6305, UK).	
	Statistical analysis	210
	All statistical analysis was performed using One-way	211
	analysis of variance (ANOVA) with the Tukey's multiple	212
	comparisons was employed for comparing the preparations	213
	with each other (Minitab [®] 16 Statistical Software). Statis-	214
	tically significant differences were assumed when $p < 0.05$.	215
	All values are expressed as their mean \pm standard	216
	deviation.	
	Results and discussions	217
	The solid-phase identity and purity of INDNIC cocrystals	218
	were verified using PXRD, DSC and FTIR prior to the	219
	inclusion complexation. The PXRD pattern and DSC	220
	melting curve and FTIR spectrum (Figs. 1a, 3a, 5a, b,	221
	respectively) of the INDNIC agreed well with the previ-	222
	ously published data [16].	223
	PXRD study	224
	The PXRD patterns of INDNIC, β -CD and their physical,	225
	co-ground and co-evaporate mixtures were presented in	226
	Fig. 1. Those with HP- β -CD, in turn, were presented in	227
	Fig. 2. The diffractograms of both INDNIC cocrystals and	228
	β -CD exhibited series of intense peaks, which are	229

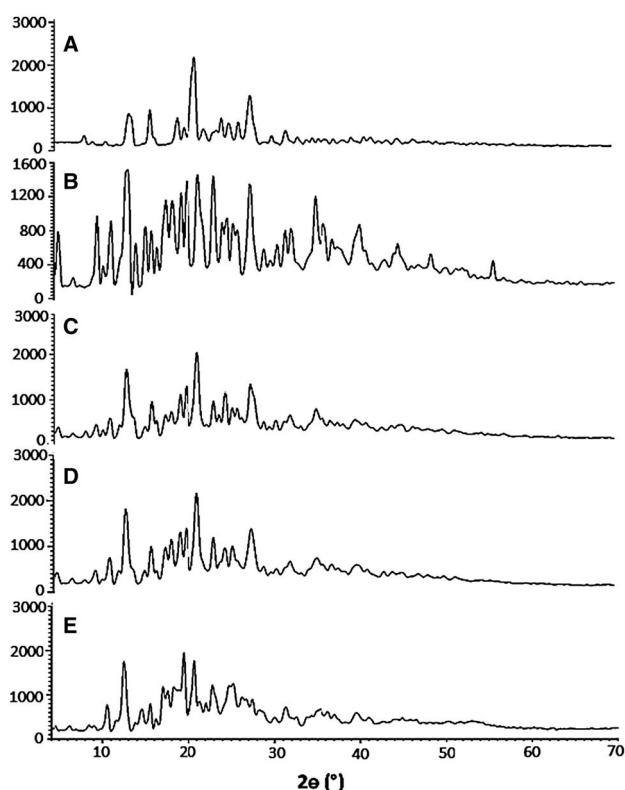


Fig. 1 The PXRD patterns of **a** INDNIC, **b** β -CD, **c** physical mixture, **(D)** co-ground mixture and **(E)** co-evaporate product. C, D and E are with β -CD

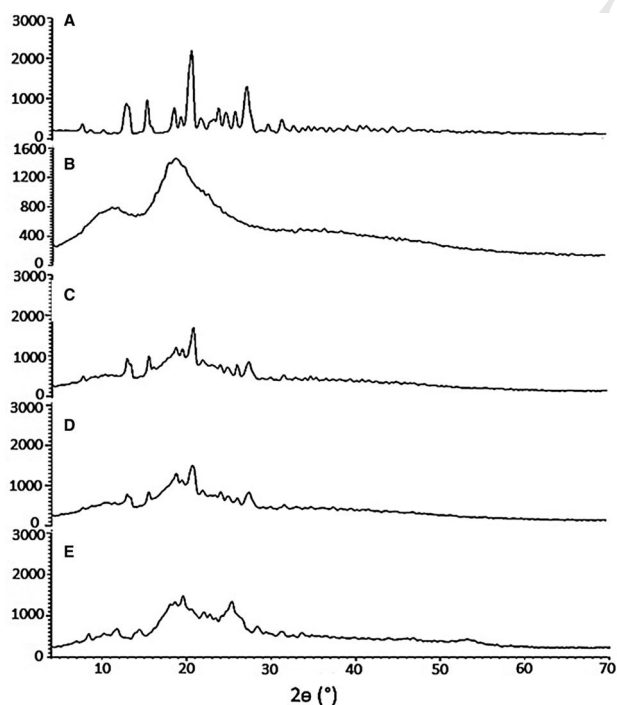


Fig. 2 The PXRD patterns of **a** INDNIC, **b** HP- β -CD, **c** physical mixture, **(D)** co-ground mixture and **(E)** co-evaporate product. C, D and E are with HP- β -CD

indicative of their crystallinity. Further, the diffractograms of their physical mixtures, co-ground mixtures still showed the characteristic peaks of both INDNIC and β -CD however, some peaks were reduced in their intensities (Fig. 1; traces C-E). Co-evaporate of INDNIC with β -CD showed further reduction in other crystalline peaks of INDNIC especially the most intense diffraction peaks at $(2\theta) = 15.35^\circ$, 23.89° and 27.22° (Fig. 1; trace D). However, the diffraction peak of INDNIC at $(2\theta) = 12.94^\circ$ was disappeared with the recording of a new diffraction peak at $(2\theta) = 12.51^\circ$ for their co-evaporate product. This may indicate that some sort of interaction has been occurred in case of the co-evaporate system which has led to formation of compound with lower crystallinity as compared with INDNIC cocrystals.

In case of INDNIC cocrystals with HP- β -CD, in turn, a significant reduction in the diffraction patterns of both the physical and co-ground mixtures of INDNIC/HP- β -CD has been observed (Fig. 2, traces C, D). On the other hand, the co-evaporate mixture of INDNIC and HP- β -CD showed new very small peaks at (2θ) values of 8.44° , 11.80° , 14.44° , 25.36° and 28.36° as compared to their physical and co-ground mixtures (Fig. 2, trace E). The disappearance of the crystalline peaks of INDNIC and recording of other new peaks could indicate the formation of structure with very low crystallinity [20]. On other words, co-evaporate system with HP- β -CD could have the potential to form an inclusion complex with INDNIC fitted inside the HP- β -CD cavity and such complex appeared to be partially amorphous.

The inclusion complexes of INDNIC with either β -CD or HP- β -CD were polycrystalline and of low crystallinity, respectively. Interestingly, Jambhekar et al. [21] concluded that, the inclusion complexes of IND itself with either β -CD or HP- β -CD were polycrystalline and amorphous, respectively.

DSC study

The DSC thermograms of INDNIC cocrystals, β -CD and their physical mixtures, co-ground and co-evaporate solid systems were presented in Fig. 3. Similarly, those with HP- β -CD were presented in Fig. 4.

The peaks corresponding to the evaporation of water vapors from both β -CD and HP- β -CD appeared at 85 and 60 $^\circ\text{C}$; respectively (Figs. 3, 4; trace B) [22, 23].

The physical and co-ground mixtures of INDNIC with β -CD showed a reduced intensity endothermic peaks at 127.73 and 127.21 $^\circ\text{C}$; respectively (Fig. 3; traces C and D) compared to that at 128.50 $^\circ\text{C}$ for INDNIC (Fig. 3; trace A). The presence of such endothermic peak in both the physical and co-ground mixtures still reflect the presence of free INDNIC in the prepared solid systems. Also, it was

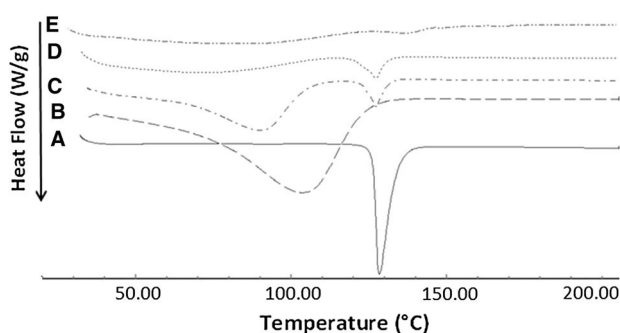


Fig. 3 The DSC thermograms of *A* INDNIC, *B* β-CD, *C* physical mixture, *D* co-ground mixture and *E* co-evaporate product. *C–E* are with β-CD

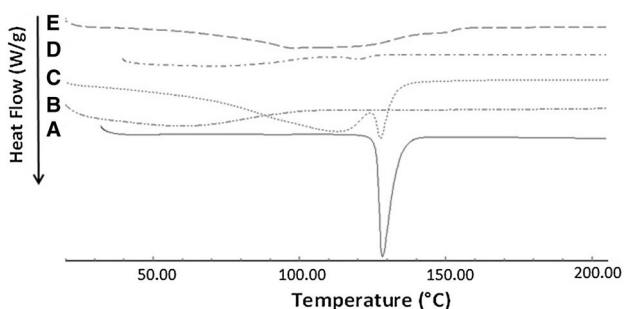


Fig. 4 The DSC thermograms of *A* INDNIC, *B* HP-β-CD, *C* physical mixture, *D* co-ground mixture and *E* co-evaporate product. *C–E* are with HP-β-CD

281 noted that the water evaporation endothermic peak was
282 shifted from 80 to 60 °C in case of the physical mixture
283 with β-CD (Fig. 3, trace C).

284 Similarly, it was found that the melting endotherm of
285 INDNIC physical and co-ground mixtures with HP-β-CD
286 appeared broader and shifted from 128.50 to 127.50 and
287 120.26 °C; respectively (Fig. 4, traces C and D). Further,
288 the broadening and reduction of that peak could be attrib-
289 uted to the incomplete complex formation via simple
290 physical and co-ground methods.

291 However, in case of co-evaporate mixtures with β-CD, a
292 small, highly broad endothermic peak was observed at
293 135.74 °C concomitantly with broadening of the water
294 evaporation peak (Fig. 3; trace E). This may indicate that
295 some sort of inclusion into the β-CD cavity was occurred
296 and there was still some INDNIC cocrystals cannot fit
297 completely inside the β-CD cavity which is responsible for
298 this small endothermic broad peak [24].

299 On the other hand, the melting endotherm of co-evap-
300 orate with HP-β-CD was completely disappeared which
301 indicated that the new solid compound formed has an
302 amorphous structure (Fig. 4; trace E). These findings come
303 in accordance with the above mentioned PXRD results.
304 Moreover, the complete disappearance of the water

evaporation peak of HP-β-CD in case of co-evaporate 305
mixture with INDNIC could indicate that the cocrystal has 306
penetrated into the HP-β-CD cavity and replaced the water 307
molecules. 308

Solid-state FTIR spectroscopic investigation 309

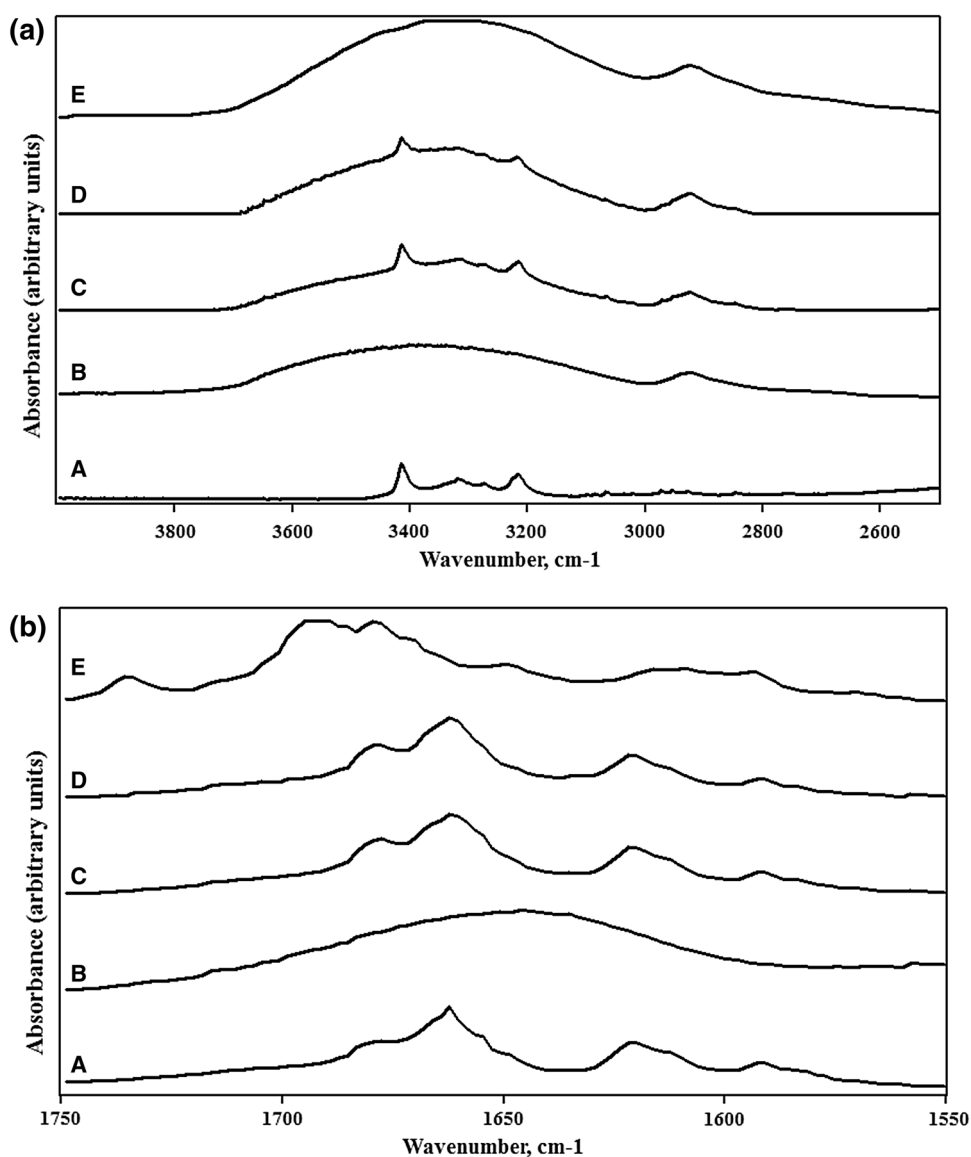
FTIR spectroscopy was used to assess the interaction 310
between the cocrystal and the two studied cyclodextrins in 311
the solid state. The chemical interaction between the host 312
and the guest molecules often leads to identifiable changes 313
in the FTIR spectra of complexes. However, some of the 314
changes are very subtle requiring careful interpretation of 315
the spectra. 316

The FTIR spectra of INDNIC, β-CD, HP-β-CD and their 317
respective physical and cog-round mixtures and co-evap- 318
orate products exhibited a number of differences in both 319
the fingerprint and high wavenumber regions (Figs. 5, 6). 320
The ν (OH) regions in the FTIR spectra appear as very 321
broad bands in the range of 3400–2500 cm⁻¹ which are 322
superimposed on the ν (CH) regions. Both the broad nature 323
and the position of these FTIR bands are characteristic of 324
hydrogen-bonded OH groups [25]. The differences in the 325
shapes of these bands suggest that there may be associated 326
variations in hydrogen bonding. 327

By close inspection of the FTIR spectra of INDNIC, β- 328
CD and their physical and ground mixtures and their co- 329
evaporate products in the wavenumber range (3400– 330
2500 cm⁻¹), it could be noted that the characteristic sharp ν 331
(OH) bands at 3413 and 3318 cm⁻¹ and ν (NH₂) bands at 332
3285 and 3218 cm⁻¹ of INDNIC were recorded as broader 333
bands in the FTIR spectra of their physical and ground 334
mixtures with reduced intensities but not in the spectrum of 335
their co-evaporate products except the ν (OH) band at 336
3413 cm⁻¹ (Fig. 5a). That may indicate incomplete inclu- 337
sion of the cocrystal in the β-CD cavity by physical mixing 338
and co-grinding approaches. The same also may apply to 339
the co-evaporation approach as indicated by the recording 340
of the above weak ν (OH) band at 3413 cm⁻¹ in the FTIR 341
spectrum of the co-evaporate product (Fig. 5a, trace E). 342
Based on the above observations, partial inclusion is more 343
efficient by the co-evaporation approach as compared to 344
the two other methods which supports the previous findings 345
from the PXRD and DSC data. 346

In case of HP-β-CD only the sharp ν (OH) and ν (NH₂) 347
bands at 3413 and 3218 cm⁻¹, respectively were recorded 348
as broader bands in the FTIR spectra of their physical and 349
ground mixtures with reduced intensities but not in the 350
spectrum of their co-evaporate products (Fig. 6a). That 351
may indicate more efficient partial inclusion of the 352
cocrystal in the HP-β-CD cavity by physical mixing and 353
co-grinding approaches. However, in case of the co- 354

Fig. 5 a The FTIR spectra in the wavenumber range (2500–4000 cm^{-1}) of *A* INDNIC, *B* β -CD, *C* physical mixture, *D* co-ground mixture and *E* co-evaporate product. *C–E* are with β -CD. **b** The FTIR spectra in the wavenumber range (1550–1750 cm^{-1}) of *A* INDNIC, *B* β -CD, *C* physical mixture, *D* co-ground mixture and *E* co-evaporate product. *C–E* are with β -CD



355 evaporation approach, the inclusion complexation appears
356 to be complete (*cf.* that with β -CD).

357 By careful inspection of the FTIR spectra of INDNIC, β -
358 CD, and their physical and ground mixtures and their co-
359 evaporate products in the wavenumber range (1550–
360 1750 cm^{-1}) region, in turn, rather interesting findings were
361 apparent (Fig. 5b). The characteristic $\nu(\text{C}=\text{O})$ bands of
362 INDNIC at 1661 and 1680 cm^{-1} were recorded in the FTIR
363 spectra of their physical and ground mixtures. However in
364 the FTIR spectrum of their co-evaporate product they were
365 shifted to 1680 and 1691 cm^{-1} , respectively with the
366 recording of a new $\nu(\text{C}=\text{O})$ band at 1735 cm^{-1} . These
367 significant shifts together with the recording of a new
368 $\nu(\text{C}=\text{O})$ band suggest the formation of new hydrogen
369 bonding between the cocrystal and the OH groups in the
370 interior cavity of β -CD during their more efficient partial

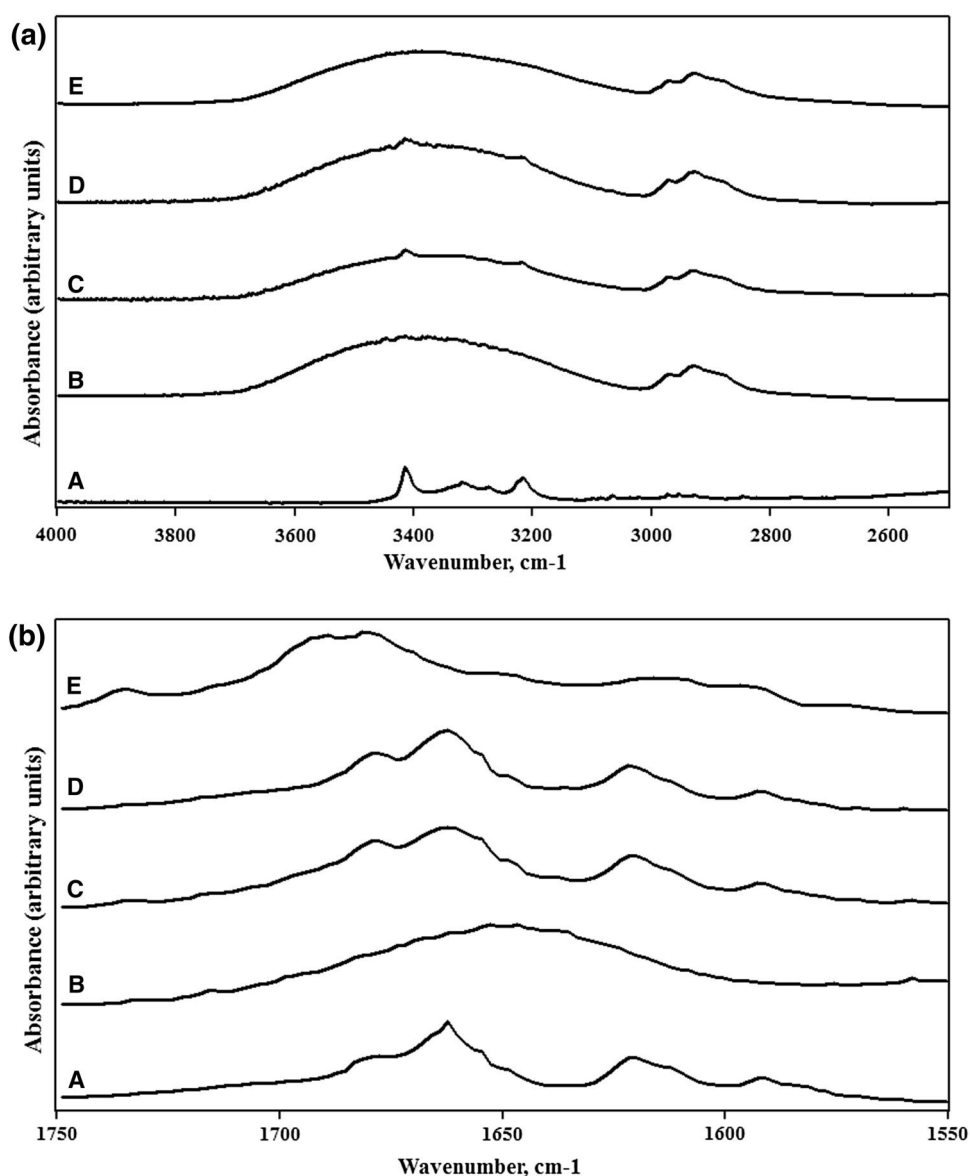
inclusion. The same was also noted with HP- β -CD 371
(Fig. 6b). These shifts together with the recording of a new 372
 $\nu(\text{C}=\text{O})$ band at 1735 cm^{-1} further confirm the complete 373
inclusion of the cocrystal with the HP- β -CD using the co- 374
evaporation approach. These findings further confirm the 375
above PXRD and DSC observations. 376

SEM analysis 377

The SEM images of INDNIC, HP- β -CD and their co- 378
evaporate and co-ground products, β -CD and its co-evap- 379
orate product with INDNIC were presented in Fig. 7 (traces 380
A, B, C D, E and F, respectively). 381

Striking differences in the morphology of the particles 382
were observed upon careful inspection of the SEM images. 383
INDNIC particles were appeared as rectangular crystals 384

Fig. 6 a The FTIR spectra in the wavenumber range (2500–4000 cm^{-1}) of *A* INDNIC, *B* HP- β -CD, *C* physical mixture, *D* ground mixture and *E* co-evaporate product. *C–E* are with HP- β -CD. **b** The FTIR spectra in the wavenumber range (1550–1750 cm^{-1}) of *A* INDNIC, *B* HP- β -CD, *C* physical mixture, *D* ground mixture and *E* co-evaporate product. *C–E* are with HP- β -CD



385 while HP- β -CD was presented as aggregated spherical
 386 particles (Fig. 7, traces A and B). By comparing the mor-
 387 phology of the co-evaporate and co-ground products of
 388 INDNIC with HP- β -CD, it could be noted that, the co-
 389 evaporate product appears as large irregular aggregates of
 390 thick lumps which differ in morphology than both INDNIC
 391 and HP- β -CD (Fig. 7, trace C), which could indicate the
 392 loss of the crystalline shape of INDNIC and formation of
 393 another complex structure with a new morphology. The co-
 394 ground product, in turn, shows the loss of the spherical
 395 appearance of HP- β -CD particles with the appearance of
 396 the cocrystals (Fig. 7, trace D). The loss of the spherical
 397 characters could be possibly attributed to the grinding
 398 process. These observations are in agreement with our

above findings from PXRD, DSC and FTIR studies which
 further confirm the complete inclusion of the cocrystal with
 the HP- β -CD using the co-evaporation approach.

To further confirm our findings, the morphology of β -
 CD particles and their co-evaporate product with INDNIC
 were also compared. Interestingly, the cocrystals were
 appeared as a huge network of aggregated filaments on the
 surface of β -CD particles (Fig. 7, trace E). Such mor-
 phology may indicate the incomplete inclusion of the
 cocrystals using the co-evaporation approach.

The variations in the particles morphology among the
 above products despite similar processing conditions could
 be explained by considerable differences in the crystal-
 lization kinetics or crystal lattices.

399
 400
 401
 402
 403
 404
 405
 406
 407
 408
 409
 410
 411
 412

Fig. 7 The SEM images of **a** INDNIC, **b** HP- β -CD, **c** co-evaporate product of INDNIC with HP- β -CD, **d** co-ground product of INDNIC with HP- β -CD, **e** β -CD and **f** co-evaporate product of INDNIC with β -CD

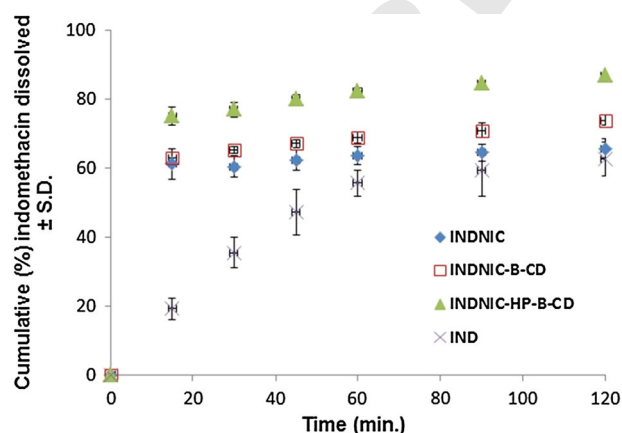
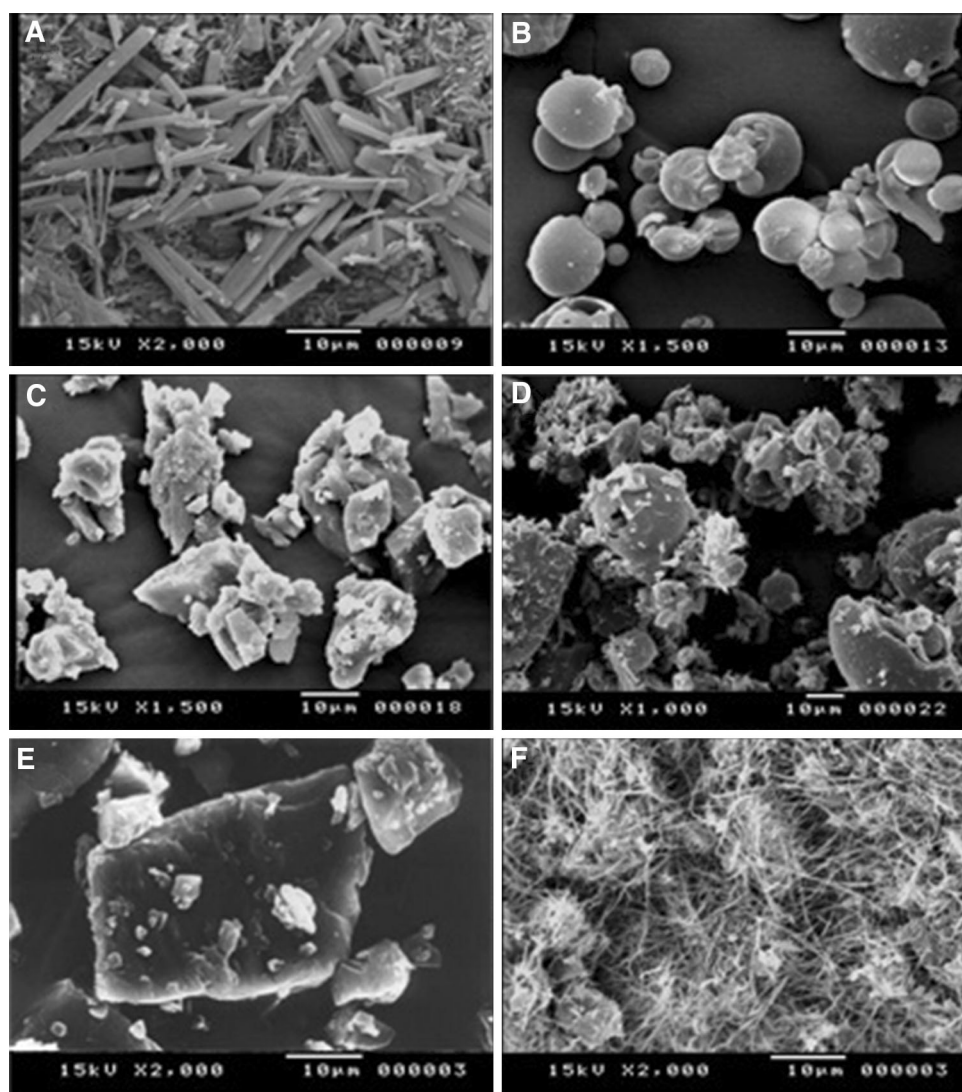


Fig. 8 The dissolution profiles of IND, INDNIC and the co-evaporate mixtures of INDNIC with β -CD and HP- β -CD

In vitro dissolution study

Figure 8 shows the dissolution profiles of IND, INDNIC and co-evaporate mixtures of INDNIC with β -CD and HP- β -CD in pH 6.8. It was found that the percentages of IND powder dissolved after 15 and 120 min were 19.32 % \pm 6.5 and 62.55 % \pm 4.9; respectively. INDNIC cocrystals and co-evaporate mixtures of INDNIC with β -CD and HP- β -CD showed a significantly ($p < 0.05$; ANOVA/Tukey) higher increase in the dissolution rate of IND 61.20 % \pm 4.5, 62.96 % \pm 1.8 and 75.16 % \pm 2.7 after 15 min; respectively compared with untreated IND powder, 19.32 % \pm 6.5, after the same time interval. Further, the co-evaporate mixture of INDNIC with HP- β -CD gives a significantly ($p < 0.05$; ANOVA/Tukey) higher increase in

413

414

415

416

417

418

419

420

421

422

423

424

425

426

427 the dissolution rate of IND 75.16 % \pm 2.7 and
 428 86.76 % \pm 0.7 after 15 and 120 min; respectively compared
 429 to INDNIC cocrystals which showed 61.20 % \pm 4.5
 430 and 65.77 % \pm 2.8 IND percentage released after the same
 431 time. INDNIC cocrystals significantly increased the dis-
 432 solution rate of IND compared with the untreated IND
 433 powder possibly as previously reported with indomethacin-
 434 saccharin cocrystals [18]. Furthermore, the effect of HP- β -
 435 CD on the dissolution rate of certain drugs was higher than
 436 that of β -CD due to its higher water solubility and the
 437 bigger capacity of its cavity [19, 26, 27]. It is worth to note
 438 that, the co-evaporate mixture with HP- β -CD produces a
 439 significant ($p < 0.05$; ANOVA/Tukey) rapid dissolution
 440 after 15 and 120 min as compared to that with β -CD co-
 441 evaporate system. That may be attributed to local solubil-
 442 isation action operating in the micro-environment or the
 443 hydrodynamic layer surrounding the cocrystals particles in
 444 the early stages of the dissolution process. Additionally,
 445 HP- β -CD dissolves in a short time compared with β -CD
 446 thus improves the wettability of the cocrystals and hence
 447 their dissolution [23]. Also, one could not neglect that, the
 448 formation of the complete inclusion complex with a new
 449 partially amorphous structure which could enhance the
 450 dissolution process compared to the co-evaporate system
 451 with β -CD and this is in agreement with PXRD, DSC and
 452 FTIR studies.

453 Conclusions

454 Partial and complete inclusion complexes of INDNIC
 455 cocrystals with β -CD and HP- β -CD were prepared suc-
 456 cessfully by the co-evaporation method in a molar ratio of
 457 1:1 of the guest to host molecules. This was confirmed by
 458 various analytical techniques. The co-evaporate mixture of
 459 INDNIC with HP- β -CD showed new morphological
 460 structure as observed from SEM Study. The prepared
 461 inclusion complexes enhanced the dissolution rate of IND
 462 significantly as compared with the untreated IND and
 463 INDNIC cocrystals. Furthermore, the highest improvement
 464 in IND in vitro dissolution was observed in the inclusion
 465 complex prepared with HP- β -CD.

467 References

- 468 1. Datta, S., Grant, D.J.W.: Crystal structures of drugs: advances in
 469 determination, prediction and engineering. *Nat. Rev. Drug Dis-*
 470 *covery* **3**(1), 42–57 (2004)
- 471 2. Aakeröy, C.B., Champness, N.R., Janiak, C.: Recent advances in
 472 crystal engineering. *CrystEngComm.* **12**(1), 22–43 (2010)
- 473 3. Almarsson, Ö., Zaworotko, M.J.: Crystal engineering of the
 474 composition of pharmaceutical phases. Do pharmaceutical

- co-crystals represent a new path to improved medicines? *Chem.*
Commun. **17**, 1889–1896 (2004) 475
4. Rodríguez-Hornedo, N., Nehm, S.J., Seefeldt, K.F., Pagan-Torres,
 Y., Falkiewicz, C.J.: Reaction crystallization of pharmaceutical
 molecular complexes. *Mol. Pharm.* **3**(3), 362–367 (2006) 476
5. Shan, N., Toda, F., Jones, W.: Mechanochemistry and co-crystal
 formation: effect of solvent on reaction kinetics. *Chem. Commun.*
20, 2372–2373 (2002) 477
6. Aakeröy, C.B., Fasulo, M.E., Desper, J.: Cocrystal or salt: does it
 really matter? *Mol. Pharmaceutics* **4**(3), 317–322 (2007) 478
7. Lenthall, J.T., Steed, J.W.: Organometallic cavitands: cation- π
 interactions and anion binding via π -metallation. *Coord. Chem.*
Rev. **251**(13), 1747–1760 (2007) 479
8. Smith, C.B., Barbour, L.J., Makha, M., Raston, C.L., Sobolev, A.
 N.: Lanthanide-induced helical arrays of [Co (III) sepulchrate] \hat{a}
 {p-sulfonatocalix [4] arene}] supermolecules. *Chem. Commun.*
9, 950–952 (2006) 480
9. Osa, T., Suzuki, I., Szejtli, J., Osa, T.: *Comprehensive Supramolecular*
Chemistry, vol. 3. Elsevier Science Ltd., Oxford (1996) 481
10. Liu, L., Guo, Q.-X.: The driving forces in the inclusion com-
 plexation of cyclodextrins. *J. Incl. Phenom. Macrocycl. Chem.* **42**
 (1–2), 1–14 (2002) 482
11. Brewster, M.E., Loftsson, T.: Cyclodextrins as pharmaceutical
 solubilizers. *Adv. Drug Deliv. Rev.* **59**(7), 645–666 (2007) 483
12. Laza-Knoerr, A.L., Gref, R., Couvreur, P.: Cyclodextrins for drug
 delivery. *J. Drug Target.* **18**(9), 645–656 (2010). doi:10.3109/
 10611861003622552 484
13. Duchêne, D.: *Cyclodextrins and Their Industrial Uses*, vol. 3. De
 Sante', Paris (1987) 485
14. Sweetman, S.C.: *Martindale: The Complete Drug Reference*.
 Pharmaceutical Press, London (2011) 486
15. Alhalaweh, A., Velaga, S.P.: Formation of cocrystals from stoi-
 chiometric solutions of incongruently saturating systems by spray
 drying. *Cryst. Growth Des.* **10**(8), 3302–3305 (2010) 487
16. Ali, H.R.H., Alhalaweh, A., Velaga, S.P.: Vibrational spectro-
 scopic investigation of polymorphs and cocrystals of
 indomethacin. *Drug Dev. Ind. Pharm.* **39**(5), 625–634 (2013) 488
17. Shikhar, A., Bommana, M.M., Gupta, S.S., Squillante, E.: For-
 mulation development of Carbamazepine \hat{a} “Nicotinamide co-
 crystals complexed with $^3\hat{c}$ -cyclodextrin using supercritical fluid
 process. *J. Supercrit. Fluids* **55**(3), 1070–1078 (2011) 489
18. Basavoju, S., Bostrom, D., Velaga, S.P.: Indomethacin-saccharin
 cocrystal: design, synthesis and preliminary pharmaceutical
 characterization. *Pharm. Res.* **25**(3), 530–541 (2008) 490
19. Abou-Taleb, A.E., Abdel-Rahman, A.A., Samy, E.M., Tawfeek, A.O.
 H.M.: Interaction of rofecoxib with β -cyclodextrin and hydrox-
 ypropyl β -cyclodextrin in solution and in solid state. *Bull. Pharm.*
Sci. Assiut Univ., **29**(Part 2) (2006) 491
20. Sanghavi, N.M., Mayekar, R., Fruitwala, M.: Inclusion com-
 plexes of terfenadine-cyclodextrins. *Drug Dev. Ind. Pharm.* **21**(3),
 375–381 (1995) 492
21. Jambhekar, S., Casella, R., Maher, T.: The physicochemical char-
 acteristics and bioavailability of indomethacin from $^2\hat{c}$ -cyclodextrin,
 hydroxyethyl- $^2\hat{c}$ -cyclodextrin, and hydroxypropyl- $^2\hat{c}$ -cyclodextrin
 complexes. *Int. J. Pharm.* **270**(1), 149–166 (2004) 493
22. Veiga, F., Fernandes, C., Maincent, P.: Influence of the preparation
 method on the physicochemical properties of tolbutamide/cyclodex-
 trin binary systems. *Drug Dev. Ind. Pharm.* **27**(6), 523–532 (2001) 494
23. Veiga, F., Teixeira-Dias, J.J.C., Kedzierewicz, F., Sousa, A.,
 Maincent, P.: Inclusion complexation of tolbutamide with β -cy-
 clodextrin and hydroxypropyl- β -cyclodextrin. *Int. J. Pharm.* **129**
 (1), 63–71 (1996) 495
24. Kim, K.H., Frank, M.J., Henderson, N.L.: Application of differ-
 ential scanning calorimetry to the study of solid drug dispersions.
J. Pharm. Sci. **74**(3), 283–289 (1985) 496

- 540
541
542
543
544
545
25. Lin-Vien, D., Colthup, N.B., Fateley, W.G., Grasselli, J.G.: The Handbook of Infrared and Raman Characteristic Frequencies of Organic Molecules. Academic Press, San Diego (1991)
26. McCandless, R., Yalkowsky, S.H.: Effect of hydroxypropyl- β -cyclodextrin and pH on the solubility of levemopamil HCl. J. Pharm. Sci. **87**(12), 1639–1642 (1998)
27. Bouchal, F.S., Skiba, M., Fatmi, S., Chaffai, N., Lahiani-Skiba, M.: Influence of the preparation method on the dissolution properties of piroxicam—cyclodextrins systems. Lett. Drug Des. Discov. **11**, 786–808 (2014)
- 546
547
548
549

UNCORRECTED PROOF

Journal : 10847

Article : 594

Author Query Form

Please ensure you fill out your response to the queries raised below and return this form along with your corrections

Dear Author

During the process of typesetting your article, the following queries have arisen. Please check your typeset proof carefully against the queries listed below and mark the necessary changes either directly on the proof/online grid or in the 'Author's response' area provided below

Query	Details Required	Author's Response
AQ1	Figures (1,2,3,5,6) are poor in quality as its labels are not readable. Please supply a new version of the said figure with legible labels preferably in .eps, .tiff or .jpeg format with 600 dpi resolution.	
AQ2	Please update Ref. [19] with page range.	